

Strong Langmuir Turbulence

Martin V. Goldman, Campus Box 391

University of Colorado

Boulder, Colorado 80309

Presented at the

U.S.-JAPAN WORKSHOP ON

STATISTICAL PLASMA PHYSICS

February 20-24, 1984

NAGOYA, JAPAN

ABSTRACT

After a brief discussion of beam-excited Langmuir turbulence in the solar wind, we explain the criteria for wave-particle, three-wave and strong turbulence interactions. We then present the results of a numerical integration of the Zakharov equations, which describe the strong turbulence saturation of a weak (low-density) high energy, bump-on-tail beam instability.

## I. Introduction

The subject of strong Langmuir turbulence has received increasing attention lately, as a result of new developments in experiment (Wong and Cheung, 1984; Leung et al., 1982; Cheung et al., 1982; Eggleston et al., 1982), two-dimensional electron-ion particle in cell simulation (Anisimov et al., 1982; Forslund et al., 1983) and statistical theory (Pelletier, 1982; Galeev et al., 1975,77). While all of these developments are pertinent to relatively strongly driven plasmas ( $|E|^2/4\pi nT \approx 0$  (0.1) where E is the amplitude of the Langmuir wave field) many of the same "strong" turbulence phenomena, such as modulational instability and Langmuir wave-packet collapse, are present at far lower wave intensities ( $|E|^2/4\pi nT \approx 0(10^{-5})$ ).

In this paper we present an analysis of strong Langmuir turbulence driven by a very weak bump-on-tail electron beam of the kind present in the solar wind during so-called "Type III" solar radio-wave emission. A complete account of the observations and plasma physics which are associated with Type III bursts can be found in the review article by the present author (Goldman, 1983).

The scenario associated with a Type III burst is illustrated in Figure 1. An electron beam is excited on the surface of the sun, possibly as a result of the release of magnetic reconnection energy during a solar flare. As the beam front progresses outwards from the sun, it excites electron plasma (Langmuir) waves. A small fraction of the Langmuir energy is nonlinearly converted into

radiation near the electron plasma frequency and near its second harmonic. It is the emission of this radiation which is called the Type III burst.

In Figure 2, we show the results of local measurements of the beam and Langmuir waves from the earth-orbiting spacecraft, ISEE-3 (Lin et al., 1981). An effective one-dimensional electron velocity distribution function is constructed, and depicted in Figure 2a at two different times. The dots represent the ambient local interplanetary plasma electron distribution function, before the arrival of the beam from the sun. The squares show the beam as a "bump" on the tail of the distribution, near  $v=c/3$ , some 35 minutes later.

Below, in Figure 2b, the Langmuir turbulence measured by the spacecraft antenna at 31 kHz is given as a function of time. The first appearance of the turbulence is simultaneous with the first appearance of the "bump-on-tail" distribution function. The quasilinear growth rate,  $\gamma$ , for this instability is about  $10^{-6}$  times the electron plasma frequency,  $\omega_p$ , so that this is a very weak instability. The measured value of the integrated wave energy density,  $W = |E|^2/4\pi nT$ , is on the order of  $10^{-5}$ .

We may study the nonlinear dynamics of a plasma driven by such a weak "bump-on-tail" electron by using the Zakharov equations in the form given below (Zakharov, 1972; Nicholson et al., 1978; Hafizi et al., 1983; Goldman, 1983).

$$(1a) \quad \nabla \cdot [i a_t + \nabla^2 - \delta n + i\gamma] \underline{E} = 0, \quad \gamma_k \approx -\alpha f_e! \omega_p/k$$

$$(1b) \quad [a_t^2 + \nabla_i a_t - c_s^2 \nabla^2] \delta n = c_s^2 \nabla^2 |E|^2$$

Here, we have employed dimensionless units in which time is measured in units of  $\omega_p^{-1}$ , distance in units of  $(2/3)^{1/2} \lambda_D$ , the Langmuir wave electric field envelope,  $E$ , in units of  $8(\pi n T)^{1/2}$ , and density in units of  $2n_0$ , where  $n_0$  is the background density. The sound speed,  $c_s^2$ , in these units is  $(3/2)(m/M)$ , where  $m$  and  $M$  are the electron and ion mass ratios, respectively.

The growth/damping rate,  $\gamma_k$ , is negative in regions of  $k$ -space which correspond to wave growth, and positive in the regions which correspond to damping. In equation (1a),  $\hat{\nabla} \cdot \mathbf{E}$  is the inverse Fourier transform of  $\gamma_k E_k$ . The term  $\hat{\nabla}_i a_c$  in equation 1b corresponds to ion-acoustic wave damping.

In equation (1a),  $\nabla^2$  corresponds to linear thermal dispersion in Langmuir waves, and  $\delta n$  to nonlinear refraction. In (1b), the density  $\delta n$  is driven by ponderomotive force, and a linear ion acoustic wave response is represented by the operator on the left side.

## II. Physical phenomenon contained in the Zakharov equations

The Zakharov equations describe a number of effects. They contain the usual three-wave "decay" interactions in which a "pump" Langmuir wave can scatter into another Langmuir wave plus an ion-acoustic wave. There is a special wavenumber in the kinematics of this scattering process, which we will call  $k_*$ :

$$k_* \approx (m/M)^{1/2} k_D$$

For a pump wavenumber much larger than  $k_*$ , the scattered Langmuir wave is always in the backward direction relative to the pump wavevector, and reduced in magnitude by the small amount  $k_*$ . For somewhat smaller pump wavenumbers,  $k_0 \gtrsim k_*$ , the scattered wave will have essentially zero wavenumber (large wavelength). For still smaller pump wavenumbers,  $k_0 < k_*$ , the three-wave interaction is no longer possible kinematically.

Let us now consider the pump wave to be one of the beam-driven waves. Its wave number is  $k_b \approx \omega_p/v_b$ , where,  $v_b$  is the beam speed. For beams which are not very energetic ( $v_b \ll \omega_p/k_*$ ), the beam-amplified pump wave backscatters. This process may continue for a number of back-and-forth scatters. At each scatter, the wave number is reduced by the amount  $k_*$ . The result is a "cascade" of wave energy to lower wavenumbers. Such cascades are well-known in "weak" turbulence, and have been observed as numerical solutions to the Zakharov equations (Nicholson and Goldman, 1978). If there is sufficient dissipation at wavenumbers lower than  $k_b$ , the beam instability can be saturated, and the resulting turbulence is termed "weak" (Kadomtsev, 1965). If there is insufficient dissipation, energy begins to build up at long wavelengths, in the so-called Langmuir wave "condensate".

Since there is usually virtually no Landau damping at very long wavelengths, the "condensate" eventually becomes unstable to the modulational instability discussed by Vedenov and Rudakov (1965). The evolution of the modulational instability involves spatially collapsing wavepackets. Modulational instability and collapse are both "strong" turbulence effects, described by the Zakharov equations. The collapse causes an eventual transfer of energy up to large  $k$ , where Landau damping provides the dissipation which saturates the instability.

For high velocity beams, we may have  $k_b$  on the order of  $k_*$ . In this case, one stimulated scatter will carry energy directly into the condensate. The Langmuir turbulence excited during Type III solar emission behaves in this way, since  $v_b \approx c/3$ .

In the Zakharov equations (1) the electron distribution function,  $f_e$ , is fixed, so there can be no reaction of the waves back on the beam particles. The Zakharov equation treatment (in this approximation) is complementary to the usual quasilinear description of a bump-on-tail electron beam, so we must ask which is the proper description. Should velocity space plateau formation be taken into account or do the wave-wave interactions described by the Zakharov equations dominate?

The answer is that the more rapid process dominates. If wave-wave interactions begin to rapidly transfer wave energy out of resonance with the beam at an early time (i.e., when the beam-excited modes contain only a small fraction of the beam energy), the beam-modes will not be sufficiently energetic to react back on the beam and remove its free energy by quasilinear diffusion. In this case, the wave-wave interactions certainly cannot be ignored, and strong turbulence may prevail.

We may formulate a rather simple criterion for whether the evolution of Langmuir waves driven by a beam are initially dominated either by wave-wave or by wave-particle interactions. The wave-wave scattering rate is given in dimensionless units, by

$$(2) \quad \gamma_{WW} \approx W/16,$$

where  $W \equiv \langle |E|^2 \rangle / 4\pi nT$ . Wave-wave scattering can only begin to depopulate the beam-resonant region of wave k-space when  $\gamma_{ww}$  is comparable to or greater than the growth rate of the beam-resonant waves,  $\gamma_b$ . This occurs at a wave energy density

$$(3) \quad W = W_{cr} \approx 16\gamma_b/\omega_p$$

If  $W_{cr}$  is significantly less than the beam energy density,  $nmv_b^2$ , (in units of the background particle energy density,  $nT$ ) then wave-wave interactions will occur instead of the wave-particle interactions which cause quasilinear plateau formation. Only in this situation is it self-consistent to introduce an unchangeable beam distribution function into the Zakharov eqns, as in (1a). We thus have as the criterion for wave-wave saturation of the instability:

$$(4) \quad 16\gamma_b/\omega_p \ll nmv_b^2/nT$$

For a bump-on-tail distribution function, the maximum growth rate of the beam modes is given by  $\gamma_b^{\max} \approx (n_b/n_e)(v_b/\Delta v_b)^2$ . Hence, the criterion (4) may be rewritten as:

$$(4a) \quad 4v_e \ll \Delta v_b$$

There are various limitations on the validity of this simple inequality. The (quasilinear) expression we have used for the maximum growth rate of the beam modes is only valid in the "warm beam" limit,  $(n_b/n_e)^{1/3} \ll \Delta v_b/v_b$ . In addition, for very high beam energy densities, the relevant wave-wave interaction for removal of beam-resonant wave energy density may be

intense modulational instability (Sudan, 1973, 1975), rather than stimulated scattering. Also, for beams sufficiently strong that  $W_{cr}$  exceeds the mass ratio,  $m/M$ , the rate of stimulated scatter is reduced from  $W$  to  $(m/M)^{1/2} \cdot W^{1/2}$  (Sudan, 1973, 1975; Papadopoulos, 1975). In these regimes, the condition (4a) is appropriately modified. However, in the example of strong turbulence we consider next,  $n_b/n_e$  is of order  $10^{-6}$ ,  $W_{cr}$  is of order  $10^{-5}$ , and (4a) is the proper criterion, and is well-satisfied.

### III. Numerical solutions to the Zakharov equations

Here, we present an unpublished numerical treatment, performed together with Dr. J. Weatherall, in which the measured velocity distribution function of Figure 2 is used to calculate  $\gamma_k$  in (1a). The beam-mode growth rate is very weak ( $\gamma_{b,max} \approx 10^{-6}$ ), and nonthermal Landau damping occurs on either side of the bump due to the nonthermal tail in the distribution function shown in Figure 1. The condition  $k_b \gtrsim k_*$  is satisfied, so scatter into a condensate is expected. The ion-acoustic waves which participate in the scattering process are heavily damped ( $\nu_{ik} \approx c_s k$ ).

A grid of 128 by 128 is employed, and the initial conditions consist of random-phased low-level wave noise. The wave evolution is exhibited in Figure 3, which shows the contours of constant  $|E_k|^2$ ,  $|E(x,y)|^2$ , and  $\delta n(x,y)$  (reading from left to right) at three different times (reading from top to bottom).

In Figure 3a, we see that the k-space energy has grown to a sufficiently high level ( $W \approx 10^{-5}$ ) that the wave-wave interaction of

stimulated scatter of beam-excited waves off ions is beginning to fill up a long wavelength condensate faster than the beam can continue to drive up the level of resonant waves. It is at this point in time that saturation begins. In Figure 3b, we see that the energy density of waves in real space still appears to carry the random phasing of amplified initial noise. The pattern is one of valleys and hills produced by the interference of these plane waves. Figure 3c shows that ion-acoustic plane waves have built up, due to the stimulated scatter. Their momentum is essentially that of the beam-resonant Langmuir waves, since the scattered Langmuir waves reside in the (zero-momentum) condensate.

Figure 3d shows the energy density of Langmuir waves in real space at a later time. Now there is evidence of a more coherent, self-focused wave-packet having formed. Its origin is presumably the modulationally unstable k-space condensate.

In Figure 3e, we are at a much later time. The condensate is fully formed, and very little energy is in resonance with the beam; the total energy of the waves has remained uniform since the previous snapshot because the rate of increase of total energy is proportional to the intensity of resonant energy. Figure 3f shows that the self-focused wave packet appears to be relatively stable and stationary. Presumably, the small amount of incoming wave energy due to the beam instability is balanced by the small amount of nonthermal Landau damping of the spectrum at low and high k. Figure 3g shows the density cavity which has been dug out by the ponderomotive force of the collapsed wave-packet. It too is stationary.

From these results we can draw several conclusions regarding the Langmuir

turbulence which underlies Type-III solar radio emission. The long wavelength condensate which forms has most of the spectral energy. There is a sizeable energy component at scale sizes of 25 km and longer, which are within the observability limitations of the spacecraft measuring apparatus. The mean energy density of the condensate agrees with observation ( $W \approx 10^{-5}$ ), and also with the wave scattering criterion, eqn (3). Preliminary estimates indicate that the condensate can give rise to the observed intensities of electromagnetic emission at the plasma frequency and its second harmonic. Collapse and cavitation occur, but although the collapsed wave packets have a high energy density, they do not have a high integrated energy.

We thus conclude that "strong" turbulence effects can be relevant even to very weakly driven plasmas, in which  $|E|^2/4\pi nT$  does not exceed  $10^{-5}$ .

#### Acknowledgements

This work was supported by the Air Force Office of Scientific Research, the National Science Foundation, the National Aeronautics and Space Administration, and the National Center for Atmospheric Research.

## REFERENCES

- Anisimov, S.I., M.A. Berezovskii, V.E. Zakharov, I.V. Petrov, and A.M. Rubenchik, 1982, 'Numerical Simulation of the Langmuir Collapse,' Novosibirsk Institute of Automation & Electrometry preprint #198.
- Cheung, P.Y., A.Y. Wong, C.B. Darrow, and S.J. Qian, 1982, Phys. Rev. Lett. 48, 1348.
- Eggleston, D.L., A.Y. Wong, and C.B. Darrow, 1982, Phys. Fluids 25, 257.
- Forslund, D., 1973, private conversations.
- Galeev, A.A., R.Z. Sagdeev, V.D. Shapiro, and V.I. Shevchenko, 1977, in Plasma Physics/Nonlinear Theory and Experiments/Nobel Symposium (Plenum, Wilhelmsson), p. 188.
- Galeev, A.A., R.Z. Sagdeev, Yu.S. Sigov, V.D. Shapiro, and V.I. Shevchenko, 1975, Sov. J. Plasma Phys. 1, 5; Fiz. Plazmy 1, 10 (1975).
- Goldman, M.V., 1983, Solar Phys. 89, 403.
- Hafizi, B., J.C. Weatherall, M.V. Goldman, and D.R. Nicholson, 1982, Phys. Fluids 25, 392.
- Kadomtsev, B.B., 1965, Plasma Turbulence (Academic Press, London). (Translated from Russian by L.C. Ronson)
- Leung, P., M.Q. Tran, and A.Y. Wong, 1982, Plasma Phys. 24, 567.
- Lin, R.P., D.W. Potter, D.A. Gurnett, and F.L. Scarf, 1981, Astrophys. J. 251, 64.
- Nicholson, D.R., and M.V. Goldman, 1978, Phys. Fluids 21, 1766.
- Nicholson, D.R., M.V. Goldman, P. Hoyng, and J. Weatherall, 1987, Astrophys. J. 223, 605.
- Papadopoulos, K., 1975, Phys. Fluids 18, 1769.
- Pelletier, G., 1982, Phys. Rev. Lett. 49, 782.
- Sudan, R.N., 1973, Proc. 6th European Conference on Controlled Fusion and Plasma Physics II.
- Sudan, R.N., 1975, IEEE Trans. Nucl. Sci. NS-22, 1736.
- Vedenov, A.A., and L.I. Rudakov, 1965, Soviet Physics Doklady 9, 1073; Doklady Akademii Nauk SSR 159, 767 (1964).
- Wong, A.Y., and P.Y. Cheung, 1984, Phys. Rev. Lett. 52, 1222.
- Zakharov, V.E., 1972, Sov. Phys. JETP 35, 908; Zh. Eksp. Teor. Fiz. 62, 1745 (1972).

## FIGURE CAPTIONS

Figure 1: Illustration of Type III solar radio emission. An electron beam propagates out from the sun after a flare and excites Langmuir waves of progressively lower frequencies. These waves are nonlinearly converted into emission at  $\omega_p$  and  $2\omega_p$ . Spacecraft which have detected the electron beam, Langmuir waves and electromagnetic emission are shown. (Goldman, 1983).

Figure 2: Results of ISEE-3 spacecraft measurements of electron beam and Langmuir waves during a Type III burst (not shown). a) Reduced one-dimensional electron velocity distribution function before (round dots) and during (square dots) the passage of the beam. b) Corresponding Langmuir turbulence, which onsets at the time of appearance of beam "bump." (Lin et al., 1981)

Figure 3: Numerical solution of Zakharov equations for beam-excited strong Langmuir turbulence, corresponding to Type III solar radio wave burst parameters. a),e) Wave energy density contours in k-space at  $t = 3.75\gamma^{-1}$  and at  $t = 14\gamma^{-1}$ , where  $\gamma$  = beam-mode growth rate. Scatter into a condensate is evident. b),d),f) Wave energy density contours in real space showing collapse of a Langmuir wave packet at  $t = 3.5\gamma^{-1}$ ,  $4.5\gamma^{-1}$  and  $14\gamma^{-1}$ . c),g) Contours of constant ion density in real space at  $t = 3.5\gamma^{-1}$  (showing ion-acoustic waves generated during scatter into the condensate) and at  $t = 14\gamma^{-1}$  showing density cavity supported by ponderomotive force of collapsed Langmuir wave packet.

TYPE III EMISSION:

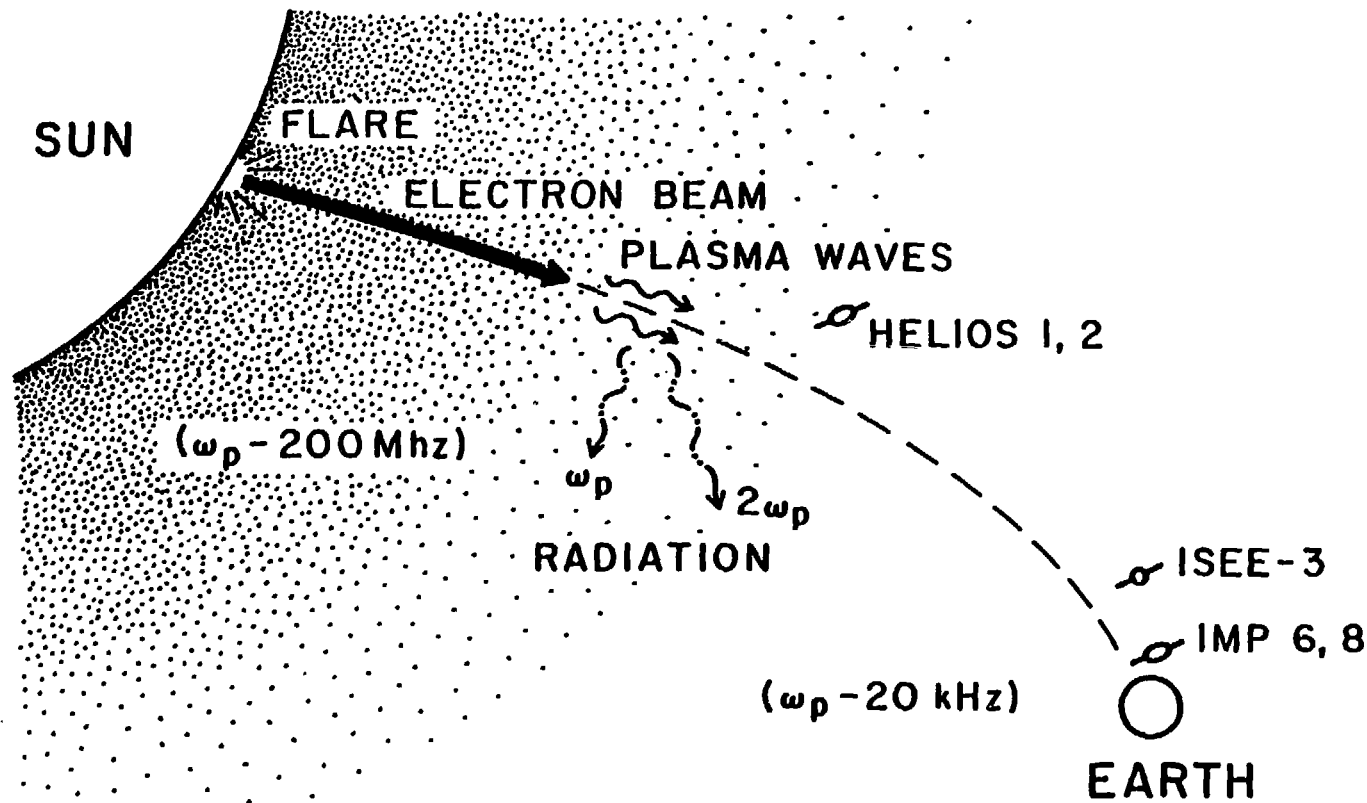
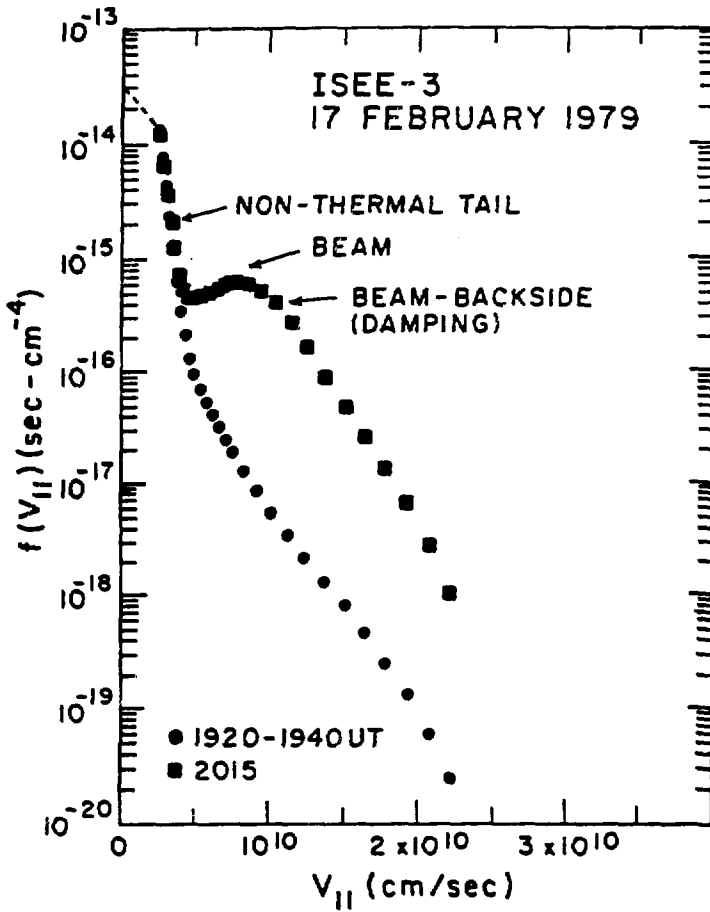


Figure 1

(a) 1-D ELECTRON DISTRIBUTION FUNCTION IN SOLAR WIND (LIN ET AL., 1981)



(b)  
LANGMUIR TURBULENCE

$w \approx 10^{-5}$

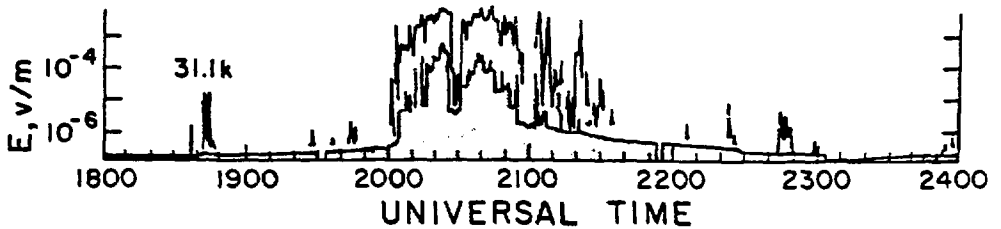


Figure 2

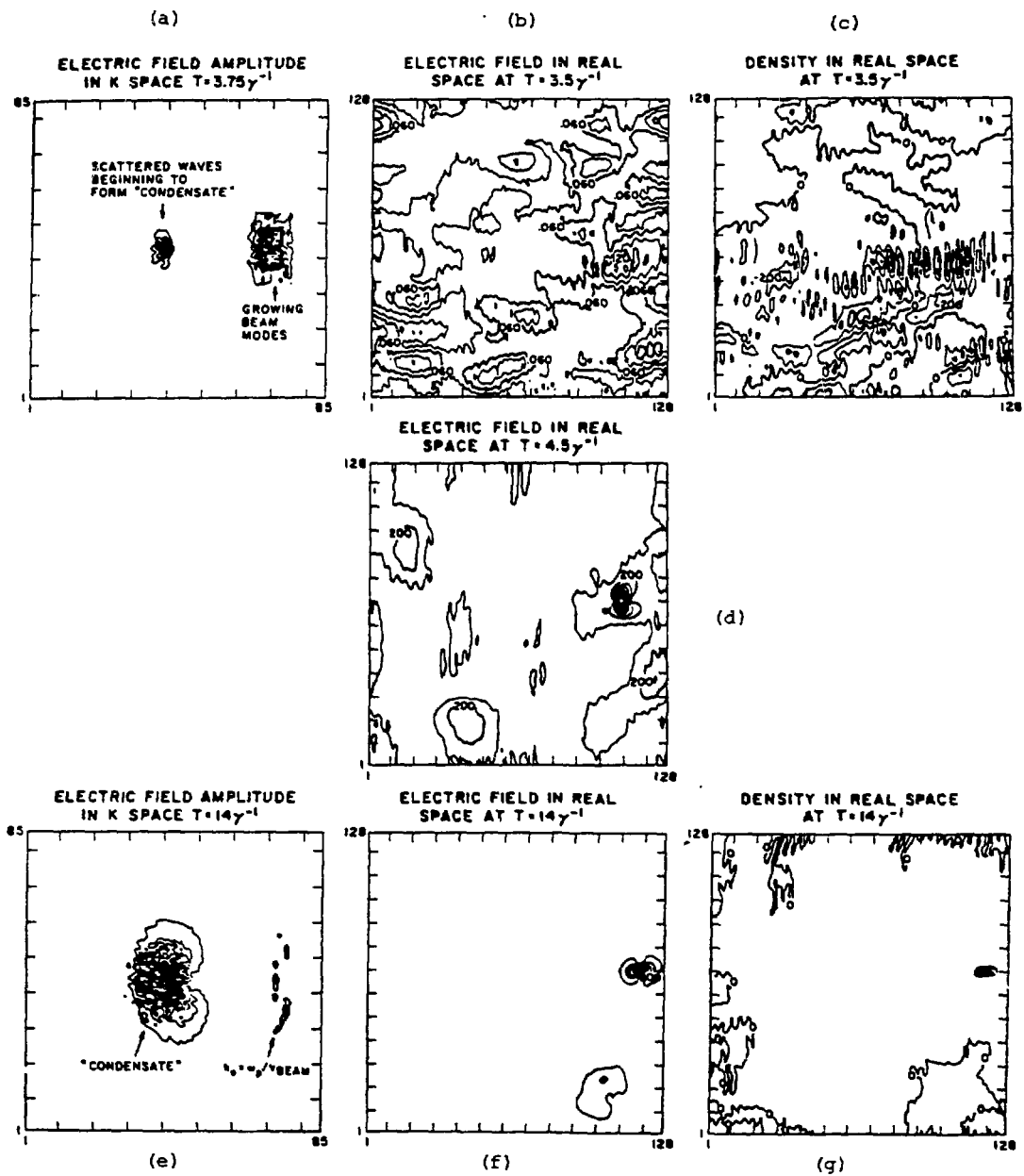


Figure 3